Electronic structure of the local-singlet insulator $NaCuO_2$

T. Mizokawa, A. Fujimori, and H. Namatame*
Department of Physics, University of Tokyo, Bunkyo-ku, Tokyo 113, Japan

K. Akeyama†
Department of Chemistry, University of Tokyo, Bunkyo-ku, Tokyo 113, Japan

N. Kosugi
Institute for Molecular Science, Myodaiji-cho, Okazaki 444, Japan
(Received 4 September 1992; revised manuscript received 12 October 1993)

The insulating oxide $NaCuO_2$ has been studied by x-ray photoemission spectroscopy and subsequent cluster-model analysis. It is found that the $d^8 \rightarrow d^9L$ charge-transfer energy (L:ligand hole) is negative and the ground state is dominated by the d^9L configuration. Using the Anderson impurity model, it is shown that strong $3d$-ligand hybridization opens a band gap for a negative charge-transfer energy. This band gap corresponds to charge fluctuations mainly of the p-p type, $d^9L + d^9L \rightarrow d^9 + d^9L^2$, with a considerable mixture of d character into the p states, and not of the conventional Mott-Hubbard (d-d) type nor of the charge-transfer (p-d) type. The magnitude of the gap is strongly affected by the geometrical arrangement of metal-oxygen local units, giving a natural explanation for the difference between the insulating $NaCuO_2$ and metallic $LaCuO_3$. The electronic structures of Fe^{4+} and Ni^{3+} oxides and their insulating versus metallic behaviors, which are expected to resemble those of the Cu^{3+} oxides, are also discussed. To generalize the above conclusions, a modification of the metal-insulator boundaries in the Zaanen-Sawatzky-Allen diagram is proposed to include compounds with small or negative charge-transfer energies.

I. INTRODUCTION

Since the discovery of high-T_c copper oxides,[1] there has been increasing interest in the electronic properties of $3d$ transition-metal compounds, where electron-electron interaction plays an important role. Recently, much work has been done on these $3d$ transition-metal compounds following interpretations of photoemission spectroscopy data[2,3] showing that photoemission spectroscopy is a powerful tool to investigate the electronic structure of these compounds.

According to the classification scheme proposed by Zaanen, Sawatzky, and Allen[3] (ZSA) based on photoemission-spectroscopy results, transition-metal compounds can be classified into two regimes according to the relative magnitudes of the ligand-to-metal charge-transfer energy Δ and the d-d Coulomb repulsion energy U. In the Mott-Hubbard regime, where $\Delta > U$, the band gap is determined by charge fluctuations of the d-d type, $d^n + d^n \rightarrow d^{n+1} + d^{n-1}$, and its magnitude is given by $\sim U$. In the charge-transfer regime, where $\Delta < U$, charge fluctuations of the type $d^n + d^n \rightarrow d^{n+1} + d^n\underline{L}$ ($\underline{L}$ = ligand hole), constitute a p-d-type band gap, whose magnitude is given by $\sim\Delta$. Systematics found in various $3d$ transition-metal compounds[4] suggest that Δ is decreased with increasing valence of the transition-metal ion and becomes very small or even negative for compounds with unusually high valence states such as Cu^{3+}, Ni^{3+}, Fe^{4+}, etc. According to the above picture, it is expected that the charge-transfer-type band gaps collapse in these compounds, leading to metallic behaviors, but actually many high-valence compounds exist as insulators.

In this paper, we have studied the electronic structure of one of the formally Cu^{3+} compounds, $NaCuO_2$. It is an insulator consisting of CuO_2 chains[5] as shown in Fig. 1. Previously Steiner *et al.* have measured the Cu $2p$ x-ray photoemission spectroscopy (XPS) spectra of $NaCuO_2$;[6] an x-ray-absorption spectroscopy (XAS) study of the Cu $2p$ core level has been reported by Sarma *et al.*[7] They have studied this compound as a reference Cu^{3+} compound in discussing the existence of Cu^{3+} species in the high-T_c copper oxide superconductors. Okada

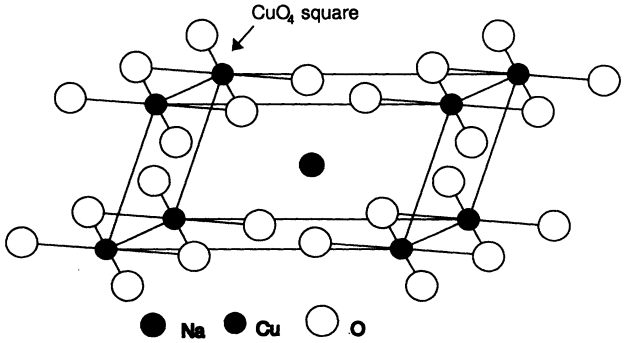

FIG. 1. Crystal structure of $NaCuO_2$. CuO_4 squares share their edges with each other and constitute CuO_2 chains.

 ©1994 The American Physical Society

et al.[8] have analyzed the Cu $2p$ XPS and XAS spectra of $NaCuO_2$ using the cluster model and estimated the charge-transfer energy Δ, although their estimated value is quite different from that deduced in the present work.

On the other hand, $LaCuO_3$ is another formally Cu^{3+} compound and is metallic. It has a rhombohedrally distorted perovskite structure but the distortion from the perovskite is very small.[9,10] There are some fundamentally important questions concerning the electronic structure of the formally Cu^{3+} oxides including both insulating $NaCuO_2$ and metallic $LaCuO_3$. One is whether the ground states of these compounds are d^8 (real Cu^{3+}) or $d^9\underline{L}$ (formally Cu^{3+} but actually Cu^{2+} plus an oxygen p hole $\underline{L}$). In the configuration-interaction theoretical scheme of charge-transfer insulators, the charge-transfer energy of Cu^{2+} oxides $\Delta(d^9 \rightarrow d^{10}\underline{L})$ has been estimated to be 1–3 eV,[11,12] and since this Δ value is smaller than the d-d Coulomb energy $U \sim 7$ eV, doped holes go into oxygen p orbitals. Therefore, it is possible that the charge-transfer energies of the formally Cu^{3+} oxides, $\Delta(d^8 \rightarrow d^9\underline{L})$, which should be smaller than those of Cu^{2+} oxides $\Delta(d^9 \rightarrow d^{10}\underline{L})$ by $\sim U$, become negative and that the $d^9\underline{L}$ configuration is dominant in the ground state. Another question is what makes the difference between the insulating $NaCuO_2$ and the metallic $LaCuO_3$. In order to answer this question, we have to elucidate the origin of the band gap in $NaCuO_2$.

In the present work, we have studied the electronic structure of $NaCuO_2$ by photoemission spectroscopy and subsequent cluster-model analysis. From the analysis, it is found that the charge-transfer energy in $NaCuO_2$ is negative and that the $d^9\underline{L}$ configuration is indeed dominant in the ground state. The difference between the insulating $NaCuO_2$ and the metallic $LaCuO_3$ is explained in terms of the relative strengths of intracluster versus intercluster hybridization, which is determined by the geometrical arrangement of the metal-oxygen local clusters. Part of the present work has already been published in previous papers,[13,14] where spectra have been analyzed using a simplified cluster model. Subsequently, the spectra were analyzed using the Anderson-impurity model by several groups,[15,16] giving general support to the picture of Refs. 13 and 14. In this paper, we present a full set of core-level and valence-band XPS spectra and detailed analyses of these as well as the XAS spectra[7] by full-multiplet cluster-model calculations. Furthermore, a modification of the Zaanen-Sawatzky-Allen diagram is presented to include the insulating compounds with small or negative charge-transfer energies in these oxides. The electronic structures of other high-valence oxides are also discussed.

The organization of this paper is as follows. Experimental details are given in Sec. II. The methods of calculations using a cluster model and an Anderson-impurity model are described in Sec. III. In Sec. IV, XPS spectra of the core levels and valence band are presented and are analyzed by the cluster-model calculations. Finally, in Sec. V, the electronic structure and the origin of the band gap of $NaCuO_2$ are investigated by using the Anderson-impurity model and their implications for related $3d$ transition-metal compounds are discussed.

II. EXPERIMENTS

Polycrystalline samples of $NaCuO_2$ were prepared by sintering a mixture of CuO and Na_2O_2 powders at 500 °C for 24 h in O_2 gas flow.[5,6] Since the samples are highly hygroscopic, the synthesis and subsequent handlings are carried out in a glove box filled with Ar gas, except for a short exposure (less than 10 sec) to air during the transfer from the glovebox to the spectrometer.

A Mg $K\alpha$ x-ray source ($h\nu = 1253.6$ eV) was used for the XPS measurements. The XPS spectra were corrected for the Mg $K\alpha_{3,4}$ ghost. Photoelectrons were collected with a PHI double-pass cylindrical-mirror analyzer. The resolution including both the x-ray source and analyzer was about 1.0 eV. In order to prevent possible loss of oxygens from the surfaces, the samples were cooled to liquid-nitrogen temperature during the measurements. Electron-energy-loss spectroscopy (EELS) measurements were also performed by using 1.7-keV incident electrons. In order to obtain fresh, clean surfaces, the samples were scraped *in situ* with a diamond file until the O 1s core-level spectrum became a single peak as shown in Fig. 2, which is an indication of good sample quality. The base pressure in the spectrometer was in the low-10^{-10}-Torr range.

III. METHOD OF MODEL CALCULATIONS

In order to analyze the XPS spectra and to obtain quantitative information about the electronic structure of

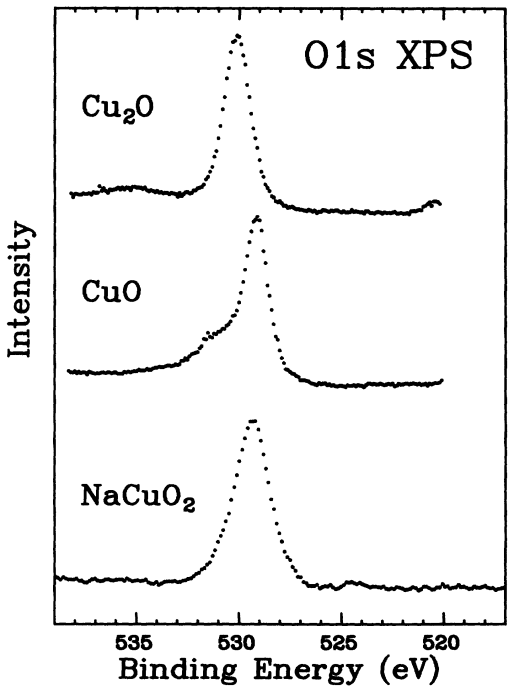

FIG. 2. O 1s XPS spectrum of $NaCuO_2$ and those of Cu_2O and CuO (Ghijsen *et al.*, Ref. 11). Ghijsen *et al.*'s spectra have been taken using monocromatized Al $K\alpha$ radiation and their resolution is 0.3–0.4 eV higher than ours.

$NaCuO_2$, we have performed configuration-interaction (CI) calculations using a square-planar $(Cu^{3+}O_4^{2-})^{5-}$ cluster model (D_{4h} symmetry).[2,8,17–20] Apart from the intra-atomic multiplet coupling and the anisotropy in the Cu-3d–ligand-p hybridization, the wave function of the ground state of the cluster is given by

$$\Psi_g = a_0|d^8\rangle + a_1|d^9\underline{L}\rangle + a_2|d^{10}\underline{L}^2\rangle \ . \quad (1)$$

We shall refer to the ground state and charge-conserving excited states as the N-electron system. The final states of 3d photoemission, namely, the eigenstates of the $(N-1)$-electron system, as given by

$$\Psi_f = b_0|d^7\rangle + b_1|d^8\underline{L}\rangle + b_2|d^9\underline{L}^2\rangle + b_3|d^{10}\underline{L}^3\rangle \ . \quad (2)$$

The lowest energy level of the $(N-1)$-electron system is the first ionization level of the N-electron system and its energy is denoted by $E_0(N-1)$. The 3d photoemission intensity is given by

$$I_f \propto |a_0b_0 + a_1b_1 + a_2b_2|^2 \quad (3)$$

in the sudden approximation. The Hamiltonian of the $(N+1)$-electron system can be constructed in an analogous way. The lowest energy level of the $(N+1)$-electron system is the affinity level of the N-electron system and its energy is denoted by $E_0(N+1)$. The magnitude of the conductivity gap in the cluster approximation is given by

$$E_{\rm gap} = E_0(N-1) + E_0(N+1) - 2E_0(N) \ . \quad (4)$$

The final states of core-level photoemission are given by

$$\Psi_f = c_0|\underline{c}d^8\rangle + c_1|\underline{c}d^9\underline{L}\rangle + c_2|\underline{c}d^{10}\underline{L}^2\rangle \ , \quad (5)$$

where $\underline{c}$ denotes a core hole. The 2p core-level photoemission intensity is given by

$$I_f \propto |a_0c_0 + a_1c_1 + a_2c_2|^2 \ . \quad (6)$$

In the calculation of the photoemission spectra, we have included both the intra-atomic multiplet coupling and the anisotropy in the 3d-ligand hybridization.[2,17] Under the D_{4h} symmetry, the Cu 3d orbitals are split into $a_{1g}(3z^2-r^2)$, $b_{1g}(x^2-y^2)$, $b_{2g}(xy)$ and $e_g(yz,zx)$ orbitals. The transfer integrals are expressed in terms of Slater-Koster parameters $(pd\sigma)$ and $(pd\pi)$.[21] At the same time, the multiplet splitting of the d^7 and d^8 configurations due to intra-atomic Coulomb and exchange interactions are taken into account through Racah parameters B and C, which have been fixed to the free-ion values.[22] In the case of $NaCuO_2$, the ground state is found to have ${}^1A_{1g}$ symmetry and the symmetries of the final states of valence-band photoemission are ${}^2A_{1g}$, ${}^2B_{1g}$, ${}^2B_{2g}$, and ${}^2E_g$. As for the core-level photoemission spectra,[8,18–20] the multiplet coupling between the core hole and 3d electrons is given in terms of Slater integrals F^2, G^1, and G^3 for the 2p and 3p core holes and G^2 for the 3s core hole.[23] We have taken the atomic values for the Slater integrals from Mann.[24]

In order to study the effect of the finite ligand bandwidth, we have used a simplified Anderson-impurity model for a Cu^{3+} ion embedded in the filled oxygen 2p band, which was employed in the analysis of the Cu 2p core-level spectra by Karlsson, Gunnarsson, and Jepsen[15] and Nimkar, Sarma, and Krishnamarthy.[16] If we follow the formulation by Zaanen and co-workers,[18,19] the wave function of the ground state of the N-electron system is given by

$$\Psi_g = \alpha\left\{|d^8\rangle + \int_{-W_p/2}^{W_p/2} d\varepsilon\,\beta(\varepsilon)|d^9\underline{L}(\varepsilon)\rangle + \int_{-W_p/2}^{W_p/2} d\varepsilon\,d\varepsilon'\gamma(\varepsilon,\varepsilon')|d^{10}\underline{L}(\varepsilon)\underline{L}(\varepsilon')\rangle\right\} , \quad (7)$$

where $\underline{L}(\varepsilon)$ denotes a ligand hole with energy ε. The matrix element between $|d^8\rangle$ and $|d^9\underline{L}(\varepsilon)\rangle$ is denoted by $\sqrt{2}V(\varepsilon)$ and that between $|d^9\underline{L}(\varepsilon)\rangle$ and $|d^{10}\underline{L}(\varepsilon')\underline{L}(\varepsilon'')\rangle$ by $\sqrt{2}V(\varepsilon'')\delta(\varepsilon-\varepsilon')$. The energy dependence of $|V(\varepsilon)|^2$ is assumed to be a semiellipsoid with an appropriate bandwidth W_p. In actual calculations, the continuum ligand band is replaced by a set of discrete states. $\int|V(\varepsilon)|^2d\varepsilon$ is taken to be equal to T^2, where $T \equiv \langle d|H|L\rangle = -\sqrt{3}(pd\sigma)$, in order to relate the Anderson-impurity model and the cluster model. In the impurity-model calculations, the intra-atomic multiplet coupling has been neglected for simplicity.

IV. EXPERIMENTAL RESULTS AND ANALYSIS

A. Core levels

In Fig. 2, the XPS spectrum of the O 1s core level is shown with those of CuO (Cu^{2+}) and Cu_2O (Cu^+) taken from Ghijsen *et al.*[11] Since $NaCuO_2$ is a good insulator, the samples were charged up during the XPS measurements and absolute binding energies could not be determined. Therefore the binding energies of the spectra of $NaCuO_2$ are tentatively calibrated so as to align the top

TABLE I. Core-level binding energies and Auger-electron kinetic energies. The energies for $NaCuO_2$ are only tentative, as described in the text. All energies given in eV.

	Cu2$p_{3/2}$ (main)		O 1s		Cu $L_3M_{45}M_{45}$
	Binding energy	FWHM	Binding energy	FWHM	Kinetic energy
Cu_2O[a]	932.4		530.2		916.8
CuO[a]	933.2		529.2		918.2
$NaCuO_2$	932.7	2.2	529.7	2.1	917.2

[a]Ghijsen *et al.* (Ref. 11).

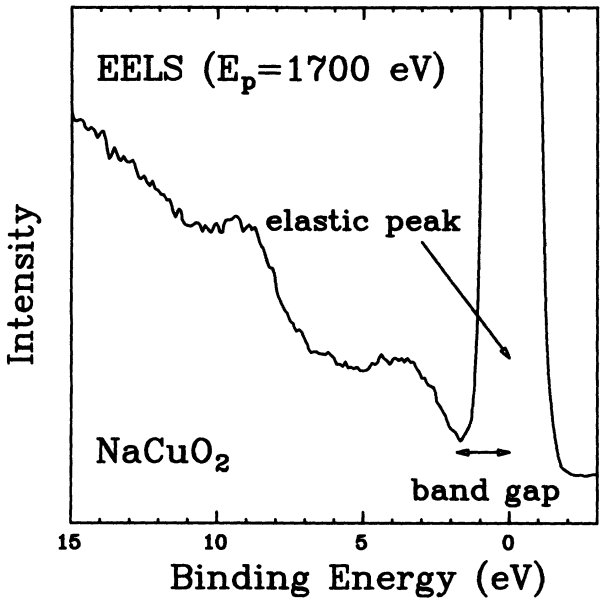

FIG. 3. EELS spectrum of $NaCuO_2$. The incident electron energy was 1.7 keV.

of the valence band with those of CuO and Cu_2O. The core-level binding energies as well as the peak widths thus determined are listed in Table I. The binding energy of the Cu $2p_{3/2}$ main peak is 0.4 eV lower than CuO, and that of the O 1*s* peak is 0.4 eV higher than that of CuO. From the EELS measurements, the band gap is found to be 1–2 eV (Fig. 3). Therefore, all the binding energies may be 1–2 eV higher than the present values if the Fermi level is located at the bottom of the conduction band, and our results do not necessarily contradict Steiner *et al.*'s results,[6] in which the binding energy of the Cu $2p_{3/2}$ main peak of $NaCuO_2$ is 1.3 eV higher than that of CuO. The full width at half maximum (FWHM) of the Cu $2p_{3/2}$ main peak is ~2.2 eV, which is much smaller than that of the Cu^{2+} compounds, ~3.2 eV. If broadening due to the inhomogeneous charging effect is taken into account, the width is also consistent with Steiner *et al.*'s results, in which the FWHM of the Cu $2p_{3/2}$ main peak is ~1.6 eV.[6] Steiner *et al.* studied $NaCuO_2$ powders pressed onto an In foil and there was no charging effect in their spectra.

We have analyzed the Cu 2*p* and 3*s* core-level spectra using the CI cluster model with and without the multiplet effect. The calculated line spectra are broadened to facilitate comparison with the experimental spectra. The Cu 2*p* and 3*s* spectra calculated without the multiplet effect are shown in Fig. 4. There are four parameters in our model, namely, Δ, U, Q, and $(pd\sigma)$. In calculating the Cu 2*p* core-level spectrum, Q is assumed to be $\sim U/0.7$ as before.[18,19] With U and Q being fixed to 7 and 10 eV, respectively, the best fit has been obtained with $\Delta=-1\pm1$ eV and $(pd\sigma)=-1.6\pm0.2$ eV. [Here, it should be noted that the Δ for core-level XPS spectra in Ref. 13 corresponds to $\Delta_{\rm eff}$ ($\sim\Delta-1.5$ eV) in this paper. For the definition of $\Delta_{\rm eff}$, see below.] The final states are decomposed into $\underline{c}d^8$, $\underline{c}d^9\underline{L}$, and $\underline{c}d^{10}\underline{L}^2$ components in Fig. 4. The $2p_{3/2}$ main peak at ~932.7 eV has mainly $\underline{c}d^{10}\underline{L}^2$ character and the satellite at ~941.5 eV has $\underline{c}d^9\underline{L}$ character. We note that it was difficult to reproduce the experimental spectrum with a positive $\Delta_{\rm eff}$ as this led to two distinct peaks in the satellite region. For the Cu 3*s* core-level spectrum, the value of the 3*s*-3*d* Coulomb attractive energy should be close to that of the 3*d*-3*d* Coulomb repulsive energy U since both orbitals have the same principal quantum number $n=3$. Actually, we could reproduce the Cu 3*s* spectrum by setting Q equal to U with the same Δ and $(pd\sigma)$ values as those of the Cu 2*p* spectrum, as shown in Fig. 4.

We have also analyzed the Cu 2*p*, 3*s*, and 3*p* core-level spectra by the cluster model including the multiplet coupling between the core hole and the 3*d* electrons. The Cu 2*p*, 3*s*, and 3*p* spectra thus calculated are shown in Figs. 5 and 6. Since the charge-transfer effect dominates the multiplet effect in the 2*p* and 3*s* spectra, the satellite structures of Cu 2*p* and 3*s* spectra are well reproduced ei-

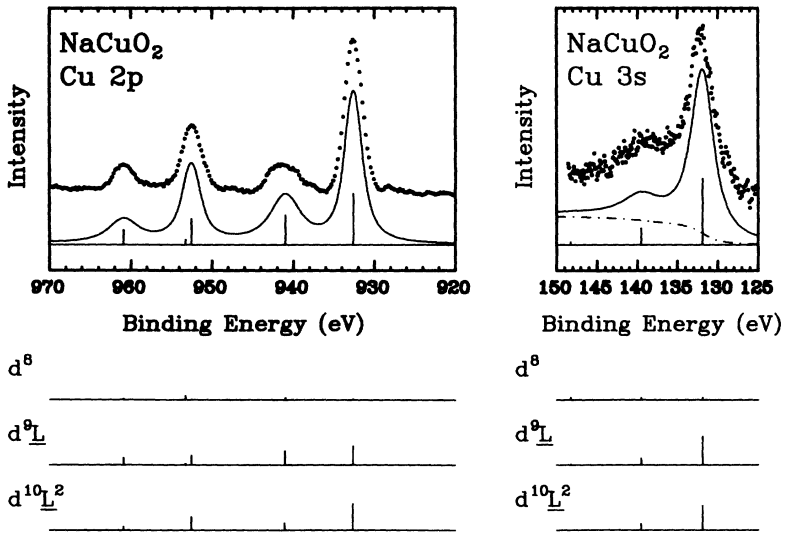

Fig. 4. Left panel: Cu 2*p* XPS spectrum of $NaCuO_2$ calculated by using the CI cluster model without multiplet coupling, and the decomposition of the line spectra into final-state configurations. The parameters are $\Delta=-1$ eV, $U=7$ eV, $T=2.9$ eV, and $Q=10$ eV. Right panel: Cu 3*s* XPS spectrum of $NaCuO_2$ calculated by using the CI cluster model, and the decomposition of the line spectra into final-state configurations. The parameters are $\Delta=-1$ eV, $U=7$ eV, $T=2.9$ eV, and $Q=7$ eV.

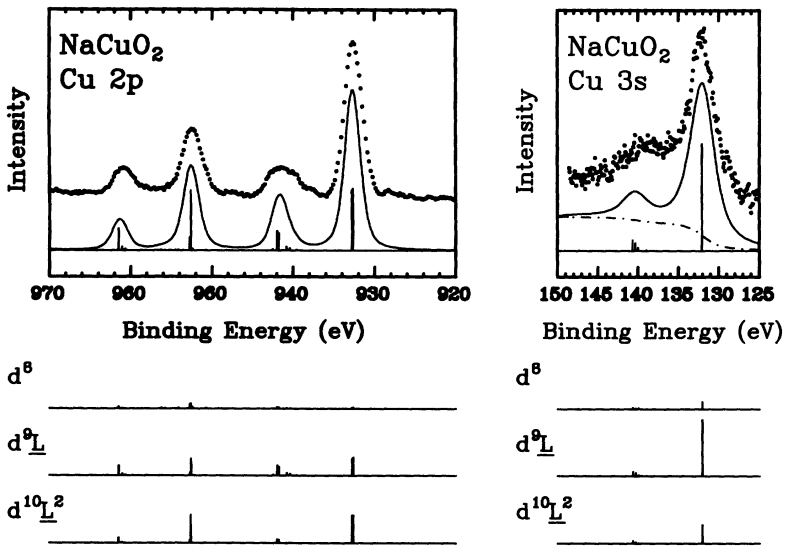

FIG. 5. Cu $2p$ XPS spectrum of $NaCuO_2$ calculated by using the CI cluster model including the multiplet coupling, and the decomposition of the line spectra into final-state configurations. The parameters are $\Delta=-2.0$ eV, $U=6.5$ eV, $(pd\sigma)=-1.8$ eV, and $F_0=8.0$ eV. $Q\equiv F^0-1/15G^1-3/70G^3\approx 7.5$ eV. Right panel: Cu $3s$ XPS spectrum of $NaCuO_2$ calculated using the CI cluster model, and the decomposition of the line spectra into final-state configurations. The parameters are $\Delta=-1.0$ eV, $U=6.5$ eV, $(pd\sigma)=-1.6$ eV, and $F^0=6.0$ eV. $Q\equiv F^0-1/10G^2\approx 4.8$ eV.

ther with or without the multiplet effect. The parameters thus obtained are close to those obtained without the multiplet effect, although there are slight differences between the two analyses: $\Delta=-2.0$ eV, $U=6.5$ eV, $(pd\sigma)=-1.8$ eV, and $Q(\equiv F^0-1/15G^1-3/70G^3)\sim 7.5$ eV for Cu $2p$, and $\Delta=-1.0$ eV, $U=6.5$ eV, $(pd\sigma)=-1.6$ eV, and $Q(\equiv F^0-1/10G^2)\sim 5.3$ eV for Cu $3s$. Here, F^0, G^1, G^2, and G^3 are Slater integrals between the Cu $2p$ and $3d$ orbitals. The values of Q are reduced by 20–30 % from those obtained by neglecting the multiplet effect. Such a tendency has also been noted by Okada *et al.*[8] On the other hand, the multiplet coupling is so strong between the $3p$ core hole and $3d$ electrons that the Cu $3p$ spectrum cannot be reproduced without including the multiplet structure.

Further, the Cu $2p$ XAS spectrum by Sarma *et al.*[7] can also be reproduced by including the multiplet effect, as shown in Fig. 7. Although fine structures due to the multiplet coupling are not evident in the calculated spectra, if we try to reproduce the spectrum without the multiplet coupling, the intensity of the satellite structure becomes too low within the reasonable parameter range. This is because in Cu $2p$ XAS, the energy difference between $\underline{c}d^n$ and $\underline{c}d^{n+1}\underline{L}$ in the final state ($n=9$) is nearly the same as that between d^n and $d^{n+1}\underline{L}$ in the initial state ($n=8$), and therefore the intensity is largely accumulated in the main peak [see Eq. (6)]. Then, the multiplet splitting causes a spread of the final states, resulting in changes in the hybridization and hence the redistribution of the spectral intensities. For the Cu $2p$ XPS, on the other hand, the level ordering of the $\underline{c}d^{n+1}\underline{L}$ and $\underline{c}d^{n+2}\underline{L}^2$ states in the final state ($n=8$) is inverted with respect to the ordering of $d^{n+1}\underline{L}$ and $d^{n+2}\underline{L}^2$ in the initial state

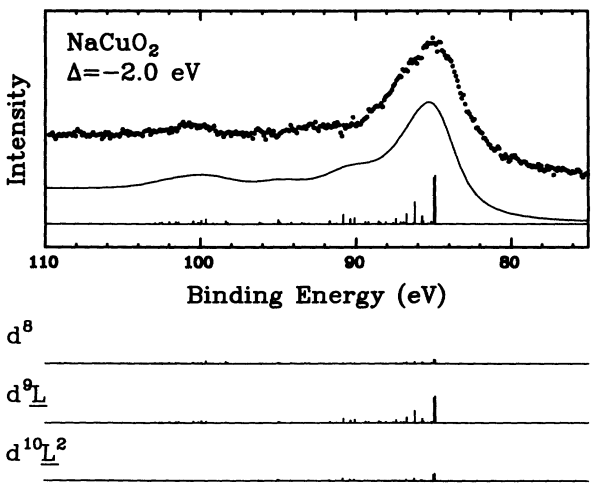

FIG. 6. Cu $3p$ XPS spectrum of $NaCuO_2$ calculated using the CI cluster model including the multiplet coupling, and the decomposition of the line spectra into final-state configurations. The parameters are $\Delta=-2.0$ eV, $U=6.5$ eV, $(pd\sigma)=-1.8$ eV, and $F_0=6.0$ eV.

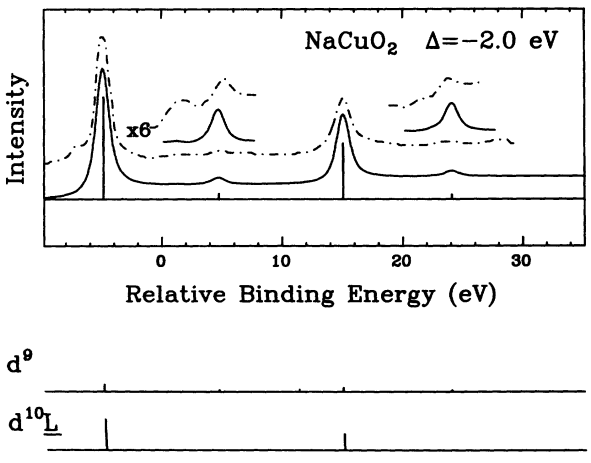

FIG. 7. Cu $2p$ XAS spectrum of $NaCuO_2$ calculated using the CI cluster model including the multiplet coupling, and the decomposition of the line spectra into final-state configurations. The calculated spectrum (solid line) is compared with the experimental result from Ref. 7 (dash-dotted line). The parameters are $\Delta=-2$ eV, $U=6.5$ eV, $(pd\sigma)=-2.0$ eV, and $F_0=9.0$ eV. $Q\equiv F^0-1/15G^1-3/70G^3\approx 8.5$ eV.

($n=8$), and the intensity of the satellite structure is rather insensitive to the multiplet splitting.

B. Valence band

In analyzing the valence-band photoemission spectrum of $NaCuO_2$, we have performed a CI calculation including the multiplet structures using a square-planar CuO_4^{5-} cluster model.[2,17] As shown in Fig. 8, when Δ is negative, the ground state is found to have $^1A_{1g}$ symmetry, where a d hole (d^9) with x^2-y^2 symmetry and a ligand hole with the same symmetry form a spin singlet, i.e., the so-called local singlet.[25,26] The ratio $(pd\sigma)/(pd\pi)$ is assumed to be ~ -2.2 as evaluated from band-structure calculations.[27,28] While the relative intensities and positions of the main band (0–6 eV) and the satellite (6–14 eV) have been well reproduced, no set of parameters in the reasonable range could reproduce the splitting of the satellite into two peaks. The spectrum shown in Fig. 9 has been calculated with $\Delta=-0.5$ eV, $U=7.0$ eV, $(pd\sigma)=-1.5$ eV. A possible origin of the discrepancy is the correlation effect between oxygen holes, which would become important with increasing $d^{n+1}\underline{L}$ contribution in the ground state but is not included in the cluster model. Further studies are necessary to clarify this point.

For the above parameter values, the ground state has 27% d^8, 65% $d^9\underline{L}$, and 8% $d^{10}\underline{L}^2$ character. This is in good agreement with *ab initio* (Hartree-Fock + CI) calculations by Akeyama and Kosugi (32.5% d^8, 61.7% $d^9\underline{L}$, 3.4% $d^{10}\underline{L}^2$).[29] In the final state of valence-band photoemission, both $d^8\underline{L}$ and $d^9\underline{L}^2$ configurations are dominant in the main band, and $d^8\underline{L}$ is dominant in the satellite region. The symmetry of the first ionization state is $^2A_{1g}$. The $d^8\underline{L}$ character of the first ionization state is slightly larger than that of $d^9\underline{L}^2$ because of the multiplet splitting of the d^8 configuration. That is, because $E[d^8(^1A_{1g})]-E[d^8(^3B_{1g})]=12B+2C=3.0$ eV, although $E[d^9\underline{L}^2]-E[d^8(^1A_{1g})\underline{L}]=\Delta+(-14/9B+7/9C)-4B-2C=-2.5\pm1$ eV is negative, $E[d^9\underline{L}^2]-E[d^8(^3B_{1g})\underline{L}]=\Delta+(-14/9B+7/9C)+8B=0.5\pm1$ eV can be positive. From the amount of the d^7, $d^8\underline{L}$, $d^9\underline{L}^2$, and $d^{10}\underline{L}^3$ character in the first ionization state (4%, 49%, 43%, and 4%, respectively), the extra hole is found to be 36% Cu d-like and 64% oxygen p-like with respect to the ground state. Likewise, the extra electron

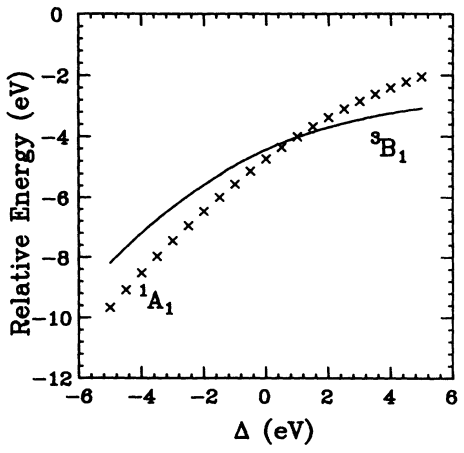

FIG. 8. Energies of the $^1A_{1g}$ (×) and $^3B_{1g}$ (solid line) states for the square-planar $(CuO_4)^{5-}$ cluster as functions of Δ for $(pd\sigma)=-1.5$ eV and $U=7.0$ eV.

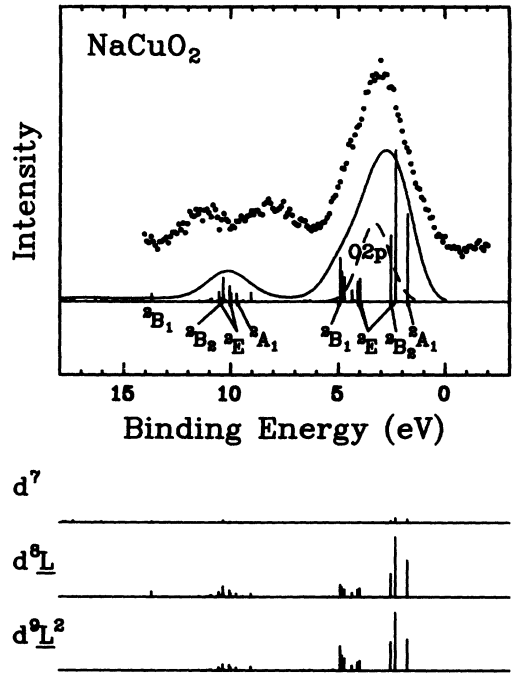

FIG. 9. Upper panel: Valence-band XPS spectra of $NaCuO_2$ calculated using the CI cluster model compared with the experimental result. Lower panel: Decomposition of the line spectrum into final-state configurations.

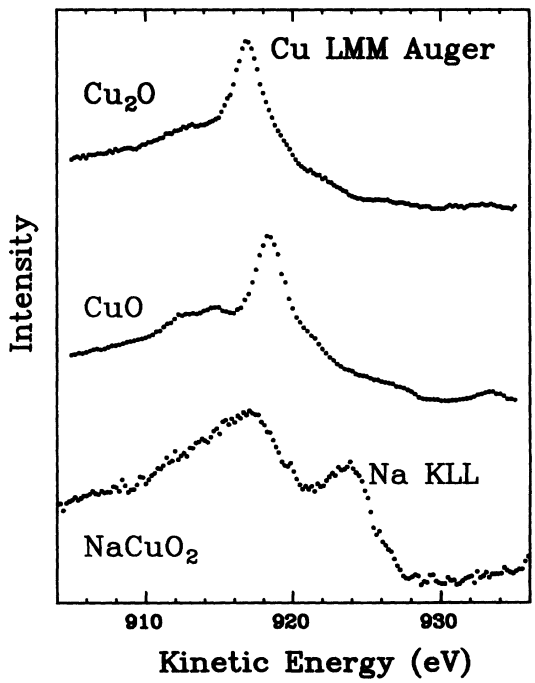

FIG. 10. X-ray-excited Auger-electron spectra of $NaCuO_2$ compared with those of CuO and Cu_2O from Ghijsen *et al.* (Ref. 11).

in the affinity level is 29% Cu d-like and 71% oxygen p-like.

C. Auger-electron spectra

In Fig. 10, the Cu $L_3M_{4,5}M_{4,5}$ Auger-electron spectrum of $NaCuO_2$ is compared with those of CuO and Cu_2O by Ghijsen *et al.*[11] For $NaCuO_2$, the main structure at $\sim$917.2 eV and the broad satellite structure at $\sim$912–916 eV mainly originate from the Cu $2p$ XAS final states corresponding to the $d^{10}\underline{L}^2$-like main peak and the $d^9\underline{L}$-like satellite, respectively. Essentially similar structures for CuO and $NaCuO_2$ is consistent with the conclusion that the ground state of $NaCuO_2$ is mainly $d^9\underline{L}$-like rather than d^8-like. The broadness of the $NaCuO_2$ spectrum is partly attributed to the lower instrumental resolution and inhomogeneous charging effects, but may also reflect the hybridized d^8 character in the ground state.

In the present energy calibration, the kinetic energy of the main structure is also intermediate between those of Cu_2O (916.8 eV) and CuO (918.2 eV), as listed in Table I.

V. DISCUSSIONS

A. Charge-transfer energies and other parameters

From the analysis of the core-level and valence-band XPS spectra, the charge-transfer energy of $NaCuO_2$ is obtained to be $\Delta\sim-1\pm1$ eV and the $d^9\underline{L}$ configuration is found to be dominant in the ground state of the Cu^{3+} compound. For Fe oxides, the Δ of FeO (Fe^{2+}) is estimated to be $\sim$6.5 eV (Ref. 30), the Δ of Fe_2O_3 (Fe^{3+}) $\sim$3.0 eV (Ref. 31) from the valence-band XPS and the Δ's of FeO, Fe_2O_3, and $SrFeO_3$ are estimated as $\sim$6.0, 3.5, and 0.0 eV, respectively, from the Fe $2p$ core-level XPS.[4,32] That is, the Δ decreases by $\sim$3 eV for a unit increase of the cation valence. Therefore, the Δ value for $NaCuO_2$ is consistent with that of Cu^{2+} oxides, 1–3 eV.[13,14]

According to the parameter estimation based on a simple ionic model,[3] $\Delta(2+)\cong\Delta V_M(2+)-I_{\rm TM}(2)+A_L(2)$, $U\cong I_{\rm TM}(3)-I_{\rm TM}(2)$, and $\Delta(3+)\cong\Delta V_M(3+)-I_{\rm TM}(3)+A_L(2)=\Delta(2+)-U+\Delta V_M(3+)-\Delta V_M(2+)$, where $\Delta V_M(2+)$ and $\Delta V_M(3+)$ are the Madelung potential difference between the transition-metal site and the oxygen site for the 2+ and 3+ compounds, respectively. Here, $I_{\rm TM}(n)$ is the nth ionization potential of the transition metal and $A_L(n)$ is the nth electron affinity of oxgyen. They are reduced from the free-ion values by screening effects due to the polarization of surrounding ions. In general, $\Delta V_M(3+)$ is larger than $\Delta V_M(2+)$ and therefore $\Delta(3+)$ is larger than $\Delta(2+)-U$ by $\Delta V_M(3+)-\Delta V_M(2+)$. From the $\Delta(3+)$, $\Delta(2+)$, and U values estimated above for the Fe or Cu oxides, we obtain $\Delta V_M(3+)-\Delta V_M(2+)\sim3$ eV. This is considerably reduced from the bare ionic values, $\sim$10 eV,[33] probably because of charge redistribution due to covalent mixing involving extended orbitals such as metal $4sp$ states.

The parameters Δ and U have been defined as $\Delta\equiv E(d^{n+1}\underline{L})-E(d^n)$, $U\equiv E(d^{n-1})+E(d^{n+1})-2E(d^n)$, where $E(d^n\underline{L}^m)$ is the center of gravity of the $d^n\underline{L}^m$ multiplet. In this definition, the multiplet effect is excluded and the systematic variation of Δ with the cation atomic number and valence becomes clear.[2,4] Alternatively, the charge-transfer energy and the d-d Coulomb interaction can also be defined with respect to the lowest term of each multiplet;[3] we denote them as $\Delta_{\rm eff}$ and $U_{\rm eff}$. The parameters $\Delta_{\rm eff}$ and $U_{\rm eff}$ rather than Δ and U should better be used when we consider the magnitudes or the character of the band gaps. In the case of low-spin $Cu^{3+}(d^8)$ compounds ($^1A_{1g}$ ground state under D_{4h} symmetry), $\Delta_{\rm eff}=\Delta+(-\frac{14}{9}B+\frac{7}{9}C)-4B-2C\cong\Delta-1.5$ eV: for $NaCuO_2$, $\Delta_{\rm eff}\sim-2.5\pm1$ eV. For high-spin $Fe^{4+}(d^4)$ compounds, $\Delta_{\rm eff}=\Delta-5(-14/9B+7/9C)-14B\cong\Delta-3$ eV:[32] for $SrFe^4+O_3$, $\Delta\sim0$ eV and hence $\Delta_{\rm eff}\sim-3$ eV.[32] Therefore, it can be said that $SrFeO_3$ (and $CaFeO_3$) also belongs to the negative-Δ (negative-$\Delta_{\rm eff}$) regime.

B. Origin of the band gap in $NaCuO_2$

According to the impurity model, neglecting hybridization between different configurations, the band gap of a charge-transfer insulator collapses and the compound becomes metallic when $\Delta_{\rm eff}$ is smaller than half of the ligand bandwidth. In the following, we consider in two steps the reason why the negative-Δ compound $NaCuO_2$ can be insulating based on the Anderson-impurity model.

In the first step, the ground state has to be a discrete state (separated by a finite energy from continuum excited states) for a system to be an insulator. The ground state of the negative-Δ compound $NaCuO_2$ consists mainly of the $d^9\underline{L}$ configuration which is originally a continuum. However, if the effect of strong hybridization is taken into account, a discrete state is split off from the continuum. It is known that the first ionization state of Cu^{2+} oxides is $d^9\underline{L}$-like with $^1A_{1g}$ symmetry and is split off from the $d^9\underline{L}$ continuum in the impurity model.[25,26] Likewise, in the ground state of $NaCuO_2$, a $d^9\underline{L}$-like discrete state will be split off from the $d^9\underline{L}$ continuum through strong hybridization with d^8 located above the $d^9\underline{L}$ continuum. In order to examine this point, we have studied the simplified Anderson-impurity model for a Cu^{3+} ion embedded in the filled oxygen band as described in Sec. III. The width of the oxygen p band $W_p=3$ eV is assumed. As shown in the bottom and middle of Fig. 11, we have indeed found that a discrete $d^9\underline{L}$-like split-off state with $^1A_{1g}$ symmetry, i.e., a local singlet, is formed $E_b(N)\sim1.5$ eV below the lower edge of the $d^9\underline{L}$ continuum for the $\Delta_{\rm eff}$, U, and $T[\equiv-\sqrt{3}(pd\sigma)]$ values obtained from the photoemission spectra. When we neglect the $d^{10}\underline{L}^2$ configuration, corresponding to the infinite-U limit, the discrete $d^9\underline{L}$-like state is also split off $\sim$1.2 and $\sim$1.4 eV below the lower edge of the $d^9\underline{L}$ continuum for the analytical (top panel of Fig. 11) and numerical (middle panel of Fig. 11) calculations, respectively.

We then have to examine whether the local singlets remain stable when the translational symmetry of the Cu-O lattice is taken into account. $NaCuO_2$ consists of edge-sharing CuO_4 square units with Cu-O-Cu bonds forming angles of nearly 90° and the wave functions of

the local singlets $d^9\underline{L}$ ($^1A_{1g}$) split off from the continuum are nearly orthogonal to those of the nearest-neighbor Cu sites, as can be seen from Fig. 12(a). Therefore, interaction between neighboring local singlets is weak and the local singlets remain localized even in the periodic lattice. Another Cu^{3+} oxide, $LaCuO_3$, which is metallic, consists of corner-sharing CuO_6 octahedra and has $\sim 180°$ Cu-O-Cu bonds. With the corner-sharing geometry, the split-off $d^9\underline{L}$ states strongly overlap with those of the nearest-neighbor clusters, as shown in Fig. 12(b), and will become extended. Namely, the formation of the split-off state is frustrated for the corner-sharing CuO_4 or CuO_6 clusters due to the strong overlap effects. (In $LaCuO_3$, a "local triplet" $^3A_{2g}$ rather than a local singlet is expected to be the ground state of the CuO_6 cluster,[25] but frustration will occur in the same way.) In a similar context, it has previously been pointed out that the geometrical arrangement of the CuO_4 clusters influences the dispersional bandwidth of the extra hole (local singlet) in Cu^{2+} oxides.[34]

In the second step, the magnitude of the band gap or the conductivity gap, i.e., the minimum energy required to create a well-separated electron-hole pair, $E_0(N+1)+E_0(N-1)-2E_0(N)(\equiv E_{\rm gap}$ in Fig. 13), has to be finite for the system to be an insulator. In general, a band gap cannot open if the ground state of the impurity model is in a continuum, but it is not sufficient for a band gap to open that the ground state is a discrete state in the impurity model. Using the above parameter values, the magnitude of the band gap is calculated to be $E_{\rm gap}\sim 1.2$ eV for the cluster model and $E_{\rm gap}\sim 0.8$ eV for the impurity model (see Fig. 13), consistent with the EELS result. The conductivity gap $E_{\rm gap}$ is smaller than the binding energy of the local singlet $E_b(N)$ by the binding energy of the discrete state in the $(N-1)$-electron state, $E_b(N-1)$. The gap mainly corresponds to charge fluctuation of the p-p type, $d^9\underline{L}+d^9\underline{L}\rightarrow d^9+d^9\underline{L}^2$, with considerable mixture of Cu d character into the oxygen p states. As described in Sec. IV A, the predominance of the p character in the states forming the band gap, particularly in the affinity level, is evident from the characters of the extra hole and electron although there is some complication arising from the multiplet splitting of the $d^8\underline{L}$ configuration. The "p-p" character of the band gap

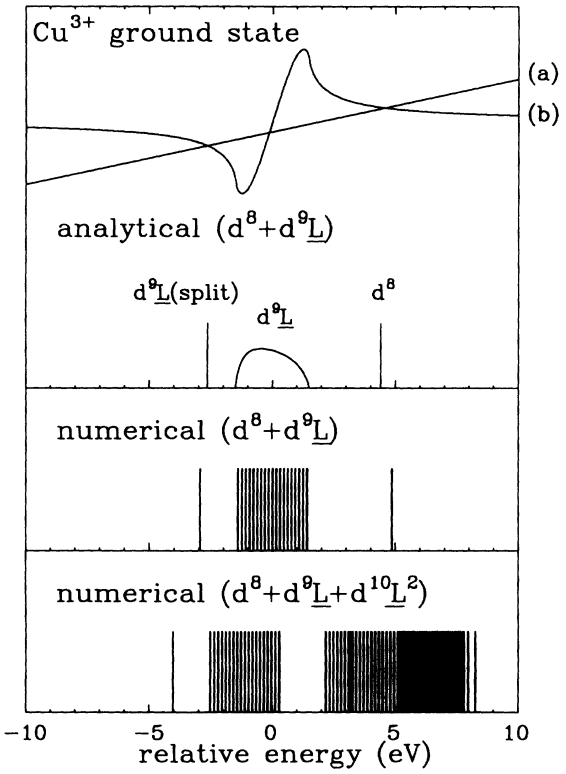

FIG. 11. Formation of a split-off state in the ground state of $NaCuO_2$. From the Anderson-impurity model neglecting the $d^{10}\underline{L}^2$ configurations, $\delta=2\int_{-W_p/2}^{W_p/2}d\varepsilon(|V(\varepsilon)|^2)/(\delta-\Delta-\varepsilon)$, where Δ is the charge-transfer energy from d^8 to $d^9\underline{L}$ and δ is the relative energy from the center of $d^9\underline{L}$. If the shape of the ligand band is assumed to be a semiellipsoid, this equation is analytically solved as shown on the top panel. Line (a) is the left-hand side of the above equation and curve (b) is the right-hand side of it. Numerical results are shown in the middle (neglecting the $d^{10}\underline{L}^2$ configuration) and at the bottom (including the $d^{10}\underline{L}^2$ configuration) by replacing the continuum band states by a set of 20 discrete states. The parameters used for the calculations are: $\Delta_{\rm eff}=-2.0$ eV, $T=2.6$ eV ($T^2\equiv\int|V(\varepsilon)|^2d\varepsilon$), $U=7.0$ eV, and the ligand bandwidth $W_p=3.0$ eV.

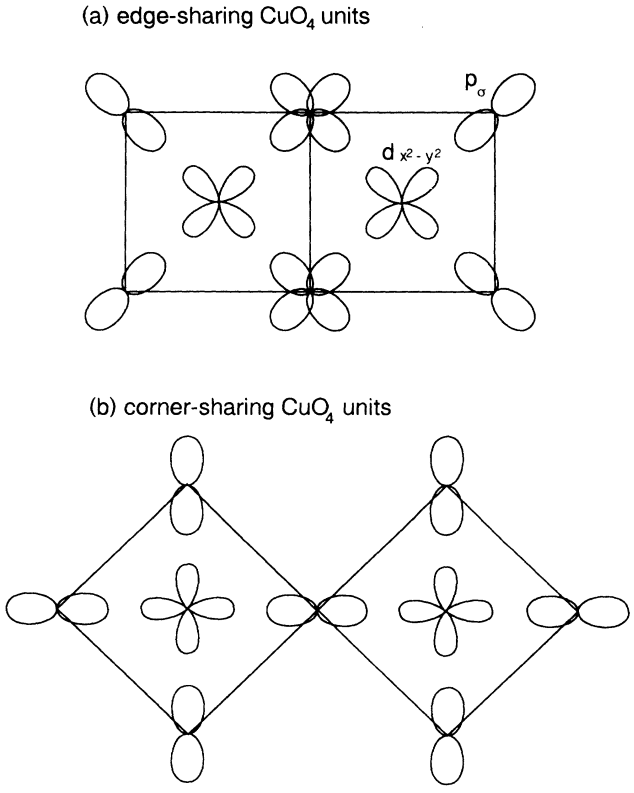

FIG. 12. (a) Edge-sharing CuO_4 units. (b) Corner-sharing CuO_4 units.

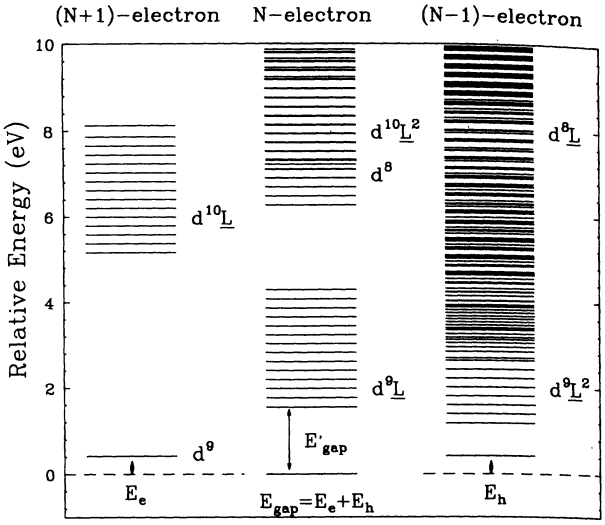

FIG. 13. Energy levels for the $(N-1)$-, N-, and $(N+1)$-electron systems calculated using the simplified Anderson-impurity model. In the N-electron system (middle), a $d^9\underline{L}$-like discrete state is split off from the bottom of the continuum. The continuum ligand band is replaced by 15 discrete states. The parameters used for the calculation are: $\Delta_{eff}=-2.0$ eV, $T=2.6$ eV, $U=7.0$ eV, and $W_p=3.0$ eV.

would be emphasized if we turn off both the p-d hybridization and the multiplet splitting. Hence, as shown in Fig. 14, the lowest affinity level corresponds to the unoccupied ligand $2p$ state hybridized with the $d_{x^2-y^2}$ state and the lowest ionization level corresponds to the occupied ligand $2p$ state heavily hybridized with the $d_{3z^2-r^2}$

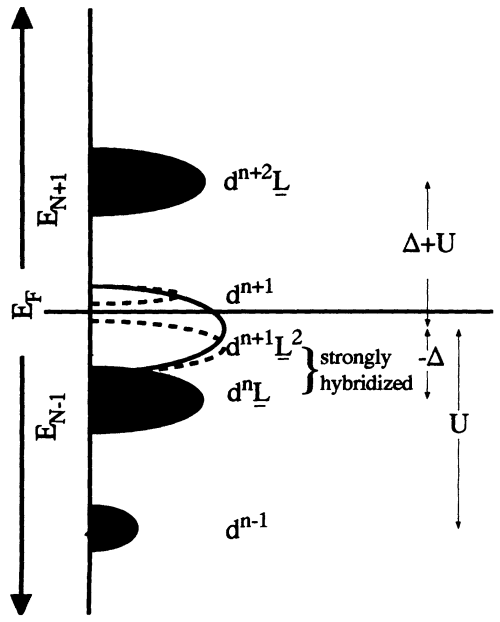

FIG. 14. Schematic representation of the single-particle spectral density for a negative-Δ insulator. The shaded and open areas represent the Cu-$3d$- and ligand-p-derived density of states, respectively. The dashed curves indicate the opening of a "p-p"-type band gap as described in the text.

state. The origin of the gap is the strong hybridization between the ligand $2p$ states and localized $3d$ states in the ground state, or the gap is opened due to the stabilization of the local singlet, i.e., the lowering of the ground-state energy $E_0(N)$ through the strong hybridization between the $d^9\underline{L}$ and d^8 configurations.

In the periodic lattice, the band gap is smaller than that predicted using the impurity model by the dispersional widths of the occupied [$(N-1)$-electron or extra-hole] and unoccupied [$(N+1)$-electron or extra-electron] states. However, both widths are expected to be small for $NaCuO_2$ because of the small overlap between the edge-sharing CuO_4 units, and the band gap will remain large even in the periodic lattice. For $LaCuO_3$, on the other hand, the band gap will be significantly reduced from the impurity value through the large dispersional width of the $(N-1)$-electron and $(N+1)$-electron states due to the corner-sharing geometry. In the single-band effective Hamiltonian obtained by Zhang and Rice,[35] which has been proposed to describe the extra holes doped into the Cu^{2+} O_2 plane as local singlets, a Cu^{3+} compound necessarily becomes an insulator since the band is thus empty. In actual Cu^{3+} compounds, however, there exists a $3z^2$-r^2 symmetry band as well as oxygen $2p$-like bands with other symmetries with which the x^2-y^2 symmetry band may overlap. Therefore, the above conditions for the formation of localized local singlets in the periodic lattice have to be satisfied for Cu^{3+} compounds to be insulating.

To summarize the above discussions, the band gap opens when the local (intracluster) p-d hybridization is strong and the extended (intercluster) hybridization is weak. That is, the magnitude of the band gap is sensitively dependent on the geometrical arrangement of the metal-oxygen local units. Now that the band gap of $NaCuO_2$ is largely due to the p-d hybridization in the ground state, it is interesting to ask whether the band gap is correctly predicted by conventional band-structure calculations. A recent band-structure calculation using the local-density approximation (LDA) by Karlsson, Gunnarsson, and Jepsen[36] has yielded a band gap of ~ 0.8 eV, comparable to our result. According to another LDA band-structure calculation by Czyzyk,[37] too, a band gap of ~ 1 eV has been obtained. Nevertheless, our cluster-model analysis shows that not only the one-electron band-structure effect but also the electron-correlation effect, i.e., the local-singlet nature of the ground state, is important in lowering the energy of the insulating ground state of $NaCuO_2$. This view is somewhat different from the recent suggestion by Sarma *et al.*[38] that Hartree-Fock calculations can predict the metallic versus insulating behaviors of negative-Δ compounds within the one-electron picture, although both approaches give qualitatively similar conditions for the band gaps to open in the negative-Δ region.

The band gap estimated here is larger than the energy difference between the $^1A_{1g}$ ground state and the lowest $^3B_{1g}$ state of the N-electron system, ~ 0.4–0.6 eV (Fig. 8). This means that a spin-flip localized excitation from the $^1A_{1g}$ to $^3B_{1g}$ state may be observed by inelastic neutron scattering.

Here, we would like to make an additional remark on

the appearance of the split-off state in the $(N+1)$-, N-, and $(N-1)$-electron systems as predicted by the impurity calculations (Fig. 13). If the bottom of the Cu 4*s* or Na 3*s* conduction band is located above the d^9 state in the $(N+1)$-electron system, the result indicates that the $Cu^{2+} \leftrightarrow Cu^{3+}$ and $Cu^{3+} \leftrightarrow Cu^{4+}$ ionization or affinity levels are located within the band gap formed between the Cu 4*s* or Na 3*s* conduction band and the O 2*p* valence band. Since the split-off ground states of the $(N+1)$, N-, and $(N-1)$-electron systems have mainly d^9, $d^9\underline{L}$, and $d^9\underline{L}^2$ characters, respectively, the successive ionization of the Cu ion is accompanied by ligand-to-3*d* charge-transfer screening with only minor decrease in the net Cu 3*d* charge. The same mechanism has been proposed by Haldane and Anderson[39] to explain the appearance of multiple charge states for transition-metal impurities in semiconductors, based on their unrestricted Hartree-Fock calculations.

C. Other high-valence oxides

As for Fe^{4+} oxides ($\Delta \sim 0$ eV, $\Delta_{\text{eff}} \sim -3$ eV), it has been reported that $SrFeO_3$ is metallic and $CaFeO_3$ is semiconducting.[40] The cubic-perovskite-type $SrFeO_3$ has 180° Fe-O-Fe bonds, whereas $CaFeO_3$ is distorted from the cubic perovskite structure with the Fe-O-Fe bond angles reduced to $\sim 150°-160°$.[40] It is possible that the band gap opens for $CaFeO_3$ in a similar way as for $NaCuO_2$, although its magnitude may be rather small. It is interesting to note that from a Mössbauer spectroscopic study, $CaFeO_3$ is proposed to undergo a transition to a charge-density-wave state involving a charge disproportionation, $2Fe^{4+} \rightarrow Fe^{3+} + Fe^{5+}$.[40] If $CaFeO_3$ belongs to the negative-Δ (negative-Δ_{eff}) regime, this charge disproportionation corresponds to charge fluctuation of the type $d^5\underline{L} + d^5\underline{L} \rightarrow d^5 + d^5\underline{L}^2$, which determines the magnitude of the band gaps of the Fe^{4+} compounds. The magnitude is so small that a small lattice distortion can make the energy of the $d^5 + d^5\underline{L}^2$ state lower than that of the $d^5\underline{L} + d^5\underline{L}$ state.

The above argument can also be applied to the electronic structure of Ni^{3+} compounds, namely, insulating $LiNiO_2$,[41] and metallic $LaNiO_3$.[42] The Δ of Ni^{2+} oxides is estimated to be ~ 4 eV (Refs. 2,43) and therefore the Δ of Ni^{3+} oxides is expected to be in the range 0–1 eV. In this case, d^7 and $d^8\underline{L}$ are nearly degenerate and are strongly hybridized with each other, leading to the formation of a split-off state in the ground state. The split-off state will still be localized and the gap persists in $LiNiO_2$ which has the NaCl structure with alternating Ni and Li (111) layers and therefore has 90° Ni-O-Ni bonds. The split-off state will be delocalized or the gap will collapse in the perovskite-structure $LaNiO_3$, where the angle of the Ni-O-Ni bond is close to 180°. More strongly distorted Ni perovskites such as $PrNiO_3$ and $NdNiO_3$ indeed show insulating gaps.[44] The opening of relatively large band gaps for small, positive Δ has been discussed by Sarma[45] in terms of strong covalency in the ground state and these compounds have been termed "covalent insulators."

D. Modification of the Zaanen-Sawatzky-Allen diagram

In the ground state of a negative-Δ insulator, the insulating state is stabilized by the formation of a chemical bond between the d^{n+1} configuration and a ligand hole within the local cluster, in a way analogous to the formation of a Heitler-London state between orbitals of neighboring atoms. In this sense, the negative-Δ insulator may be called a "valence-bond insulator," particularly for $NaCuO_2$, whose ground state is a collection of local singlets. Such insulators are contrasted with the basically ionic Mott-Hubbard and charge-transfer insulators.

In order to obtain a more general picture of the formation of band gaps for negative Δ, we have studied the magnitude of the band gaps by using the Anderson-impurity model for various sets of Δ_{eff}, U_{eff}, $T[\equiv -\sqrt{3}(pd\sigma)]$, and W_p values. In the Mott-Hubbard regime, the magnitude of E_{gap} is proportional to the *d-d* Coulomb interaction U_{eff}; in the charge-transfer regime, it is proportional to the charge-transfer energy Δ_{eff}. In the negative-Δ regime, as the ligand bandwidth W_p decreases or the effective transfer integral T increases, the band gap tends to increase. In this region, the magnitude of the band gap is proportional neither to Δ_{eff} nor to U_{eff} but sensitively depends on the hybridization strength. In order to show the dependence of the band gap on the model parameters, we plot in Fig. 15 sets of U_{eff} and Δ_{eff} values which give $E_{\text{gap}} = 0.4$ eV in the Δ_{eff}-U_{eff} plane. We may regard the $E_{\text{gap}} = 0.4$ eV line as the "metal-insulator" phase boundary, since the band gap in the periodic lattice will close for a finite E_{gap} because of the dispersional widths of the $(N+1)$- and $(N-1)$-electron systems. Then the right-hand side of the line ($E_{\text{gap}} > 0.4$

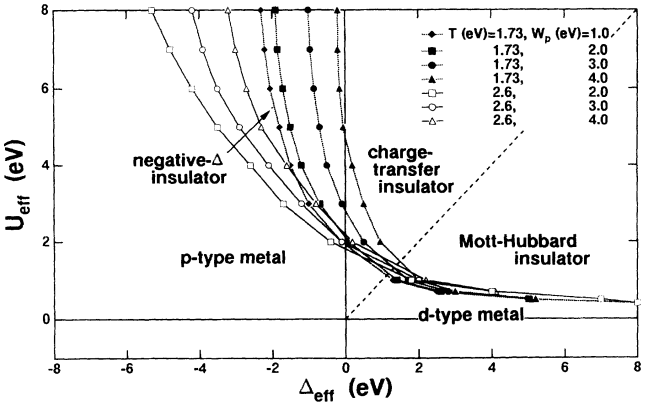

FIG. 15. Modified Zaanen-Sawatzky-Allen diagram. The curves show the "metal-insulator" phase boundaries on which the band gap E_{gap} in the impurity-model calculation is equal to 0.4 eV. The ligand bandwidth W_p and T ($T^2 \equiv \int |V(\varepsilon)|^2 d\varepsilon$) are varied as shown in the figure. The right-hand side of the curve is the "insulating" ($E_g > 0.4$ eV) phase and the left-hand side of the line is the "metallic" ($E_g < 0.4$ eV) phase. As W becomes smaller or T becomes larger, the phase boundary shifts into the negative-Δ_{eff} region. The d^8 configuration is implicitly assumed for the ground state.

eV) represents the insulating region and the left-hand side of the line ($E_{gap} < 0.4$ eV) the metallic region. As W_p becomes smaller or T becomes larger, the insulating regime is extended into the negative-Δ_{eff} region.

In a periodic lattice, d orbitals at neighboring transition-metal atoms share intervening oxygen p orbitals, which will effectively decrease the $3d$-ligand hybridization T. Also, the dispersional widths of the $(N-1)$- and $(N+1)$-electron states will effectively increase the ligand bandwidth W_p. Therefore, the effect of the intercluster hybridization may be approximately taken into account through a decrease in T and/or an increase in W_p. Consequently, the intercluster hybridization will shift the metal-insulator boundary to larger Δ_{eff}, reducing the insulating regime. The intracluster hybridization represented by the increase in T, on the other hand, will shift the boundary to smaller Δ_{eff} and extend the insulating regime. The critical E_{gap} value is actually dependent on the model parameters in a complicated way, since the dispersional widths giving the critical E_{gap} value will be affected by both the intracluster and intercluster hybridization. In order to obtain more realistic phase boundaries, the dependence of the critical E_{gap} value on the model parameter has to be taken into account. When the width of the ligand band W_p is much larger than the effective transfer integral T (for example, $W_p = 4.0$ eV and $T = 1.73$ eV), the phase boundaries lie in the positive-Δ_{eff} region and become close to those originally proposed by ZSA.[3]

VI. CONCLUSION

It is found that the Δ_{eff} of $NaCuO_2$ is ~ -2 eV, and the $d^9\underline{L}$ configuration is dominant in the ground state. The magnitude of the "p-p" band gap is related neither to U nor to Δ in a direct way and is sensitive to the relative strengths of the intracluster and intercluster hybridization. In order to fully understand the insulating versus metallic behavior of $NaCuO_2$ and $LaCuO_3$, as well as those of other high-valence transition-metal compounds, the translational symmetry of the $3d$ states as well as their correlated electronic states must be somehow taken into account more appropriately beyond the impurity limit.

ACKNOWLEDGMENTS

The authors would like to thank H. Kondoh for collaboration in the early stage of this work and O. Gunnarsson, J. C. Fuggle, G. A. Sawatzky, H. Eskes, M. T. Czyzyk, D. D. Sarma, A. Kotani, and K. Okada for useful discussions. All the calculations in this work were performed on a VAX computer in Meson Science Laboratory, Faculty of Science, University of Tokyo. The present work is supported by a Grant-in-Aid for Scientific Research from the Ministry of Education, Science and Culture and Toray Science Foundation.

---

*Present address: Department of Materials Science, Hiroshima University, Higashi-Hiroshima 724, Japan.

†Present address: Kawasaki Steel Co., Ltd., Makuhari Techno-Garden B5, Nakase, Chiba 261-01, Japan.

[1] J. G. Bednorz and K. A. Müller, Z. Phys. B **64**, 189 (1986).

[2] A. Fujimori and F. Minami, Phys. Rev. B **30**, 957 (1984).

[3] J. Zaanen, G. A. Sawatzky, and J. W. Allen, Phys. Rev. Lett. **55**, 418 (1985); J. Zaanen and G. A. Sawatzky, Can. J. Phys. **65**, 1262 (1987); J. Solid State Chem. **88**, 8 (1990); S. Hüfner, Z. Phys. B **61**, 135 (1985).

[4] A. E. Bocquet, T. Mizokawa, T. Saitoh, H. Namatame, and A. Fujimori, Phys. Rev. B **46**, 3771 (1992).

[5] K. Hestermann and R. Hoppe, Z. Anorg. Allg. Chem. **367**, 261 (1969).

[6] P. Steiner, V. Kinsinger, I. Sander, B. Siegwart, S. Hüfner, C. Politis, R. Hoppe, and H. P. Müller, Z. Phys. B **67**, 497 (1987).

[7] D. D. Sarma, O. Strebel, C. T. Simmons, U. Neukirch, G. Kaindl, R. Hoppe, and H. P. Müller, Phys. Rev. B **37**, 9784 (1988).

[8] K. Okada, A. Kotani, B. T. Tole, and G. A. Sawatzky, Solid State Commun. **77**, 835 (1991). Their definition of $\Delta[\equiv E(d^{10}\underline{L}^2) - E(d^9\underline{L})]$ is different from ours $[\Delta \equiv E(d^9\underline{L}) - E(d^8) \sim E(d^{10}\underline{L}^2) - E(d^9\underline{L}) - U]$; hence their conclusion that $\Delta < 0$ would lead to a ground state dominated by the $d^{10}\underline{L}^2$ configuration.

[9] G. Demazeau, C. Parent, M. Pouchard, and P. Hagenmuller, Mater. Res. Bull. **7**, 913 (1972).

[10] A. W. Webb, E. F. Skelton, S. B. Qadri, E. R. Carpenter, Jr., M. S. Osofsky, R. J. Soulen, and V. LeTourneau, Physica C **162**, 899 (1989).

[11] J. Ghijsen, L. H. Tjeng, J. van Elp, H. Eskes, J. Westerink, G. A. Sawatzky, and M. T. Czyzyk, Phys. Rev. B **38**, 11 322 (1988).

[12] A. Fujimori, S. Takekawa, E. Takayama-Muromachi, Y. Uchida, A. Ono, T. Takahashi, Y. Okabe, and H. Katayama-Yoshida, Phys. Rev. B **39**, 2255 (1989).

[13] T. Mizokawa, H. Namatame, A. Fujimori, K. Akeyama, H. Kondoh, H. Kuroda, and N. Kosugi, Phys. Rev. Lett. **67**, 1638 (1991); **70**, 1565(E) (1993).

[14] T. Mizokawa, H. Namatame, A. Fujimori, H. Eisaki, S. Uchida, K. Akeyama, H. Kuroda, H. Kondoh, and N. Kosugi, Physica C **185-189**, 1053 (1991).

[15] K. Karlsson, O. Gunnarsson, and O. Jepsen, J. Phys. Condens. Matter **4**, 2801 (1992).

[16] S. Nimkar, D. D. Sarma, and H. R. Krishnamurthy, Phys. Rev. B **47**, 10 927 (1993).

[17] H. Eskes, L. H. Tjeng, and G. A. Sawatzky, Phys. Rev. B **41**, 288 (1990).

[18] J. Zaanen, C. Westra, and G. A. Sawatzky, Phys. Rev. B **33**, 8060 (1986).

[19] J. Zaanen, Ph.D. thesis, University of Groningen, 1986.

[20] G. van der Laan, C. Westra, C. Haas, and G. A. Sawatzky, Phys. Rev. B **23**, 4369 (1981).

[21] J. C. Slater and G. F. Koster, Phys. Rev. **94**, 1498 (1954).

[22] S. Sugano, Y. Tanabe, and H. Kamimura, *Multiplets of Transition Metal Ions in Crystals* (Academic, New York, 1970).

[23] J. C. Slater, *Quantum Theory of Atomic Spectra I, II*

(McGraw-Hill, New York, 1960).
[24]J. B. Mann (unpublished).
[25]H. Eskes and G. A. Sawatzky, Phys. Rev. Lett. **61**, 1415 (1988).
[26]A. Fujimori, Phys. Rev. B **39**, 793 (1989).
[27]W. A. Harrison, *Electronic Structure and the Properties of Solids* (Dover, New York, 1989).
[28]L. F. Mattheiss, Phys. Rev. B **5**, 290 (1972).
[29]K. Akeyama and N. Kosugi (unpublished).
[30]The Δ of FeO has been interpolated between MnO [A. Fujimori, F. Minami, K. Siratori, M. Taniguchi, and S. Suga, Phys. Rev. B **42**, 7580 (1990)] and NiO (Ref. 2).
[31]A. Fujimori, M. Saeki, N. Kimizuka, M. Taniguchi, and S. Suga, Phys. Rev. B **34**, 3318 (1986).
[32]A. E. Bocquet, A. Fujimori, T. Mizokawa, T. Saitoh, H. Namatame, S. Suga, N. Kimizuka, Y. Takeda, and M. Takano, Phys. Rev. B **45**, 1561 (1992).
[33]J. B. Torrance, P. Lacorre, C. Asavaroengchai, and R. M. Metzger, J. Solid State Chem. **90**, 168 (1991).
[34]O. Gunnarsson, O. Jepsen, and Z.-X. Shen, Phys. Rev. B **42**, 8707 (1990).
[35]F. C. Zhang and T. M. Rice, Phys. Rev. B **37**, 3759 (1988).
[36]K. Karlsson, O. Gunnarsson, and O. Jepsen (private communication).
[37]M. T. Czyzyk (private communication).
[38]D. D. Sarma, H. R. Krishnamurthy, S. Nimkar, S. Ramasesha, P. P. Mitra, and T. V. Ramakrishnan, Pramana **38**, L531 (1992).
[39]F. D. M. Haldane, and P. W. Anderson, Phys. Rev. B **13**, 2553 (1976).
[40]M. Takano and Y. Takeda, Bull. Inst. Chem. Res. Kyoto Univ. **61**, 406 (1983).
[41]K. Hirakawa, H. Kadowaki, and K. Ubukoshi, J. Phys. Soc. Jpn. **54**, 3526 (1985).
[42]J. B. Goodenough and P. Raccah, J. Appl. Phys. **36**, 1031 (1965).
[43]H. Eisaki, S. Uchida, T. Mizokawa, H. Namatame, A. Fujimori, J. van Elp, P. Kuiper, G. A. Sawatzky, S. Hosoya, and H. Katayama-Yoshida, Phys. Rev. B **45**, 12 513 (1992); P. Kuiper, J. van Elp, G. A. Sawatzky, A. Fujimori, and D. M. de Leeuw, Phys. Rev. B **44**, 4570 (1991).
[44]J. B. Torrance, P. Lacorre, A. I. Nazzal, E. J. Ansaldo, and Ch. Niedermayer, Phys. Rev. B **45**, 8209 (1992).
[45]D. D. Sarma, J. Solid State Chem. **88**, 45 (1990).